Physics Letters A 374 (2010) 3487–3490

Contents lists available at ScienceDirect

Physics Letters A

www.elsevier.com/locate/pla

Stirring by swimming bodies

Jean-Luc Thiffeault [a,b,*], Stephen Childress [c]

[a] Department of Mathematics, University of Wisconsin – Madison, 480 Lincoln Dr., Madison, WI 53706, USA
[b] Institute for Mathematics and Applications, University of Minnesota – Twin Cities, 207 Church Street S.E., Minneapolis, MN 55455, USA
[c] Courant Institute of Mathematical Sciences, New York University, 251 Mercer Street, New York, NY 10012, USA

ARTICLE INFO

Article history:
Received 17 June 2010
Accepted 18 June 2010
Available online 23 June 2010
Communicated by C.R. Doering

Keywords:
Biomixing
Chaotic mixing
Enhanced diffusion

ABSTRACT

We consider the stirring of an inviscid fluid caused by the locomotion of bodies through it. The swimmers are approximated by non-interacting cylinders or spheres moving steadily along straight lines. We find the displacement of fluid particles caused by the nearby passage of a swimmer as a function of an impact parameter. We use this to compute the effective diffusion coefficient from the random walk of a fluid particle under the influence of a distribution of swimming bodies. We compare with the results of simulations. For typical sizes, densities and swimming velocities of schools of krill, the effective diffusivity in this model is five times the thermal diffusivity. However, we estimate that viscosity increases this value by two orders of magnitude.

Munk [1] was the first to ask whether biology has an important impact on mixing in the oceans. Since mixing affects the global circulation and stratification of the oceans, it is of great interest to physical oceanographers to settle this question. Dewar et al. [2] have proposed that the mechanical energy delivered by the swimming motions of the marine biosphere could amount to almost 10^{12} W, a figure comparable to the energy delivered by the winds and tides. This suggests a biological origin of about 33% of the mixing in the oceans, an enormous figure. By assuming that this energy is delivered to the top three kilometers of the oceans, they estimate an effective diffusivity produced by swimmers to be approximately .2 $\mathrm{cm}^2/\mathrm{sec}$, or about 100 times the molecular value for heat. Kunze et al. [3] have measured elevated levels of ocean turbulence due to swimming krill, though some have questioned whether this turbulence can efficiently overturn a stratified medium [4,5]. Katija and Dabiri [6] suggest that the displacement of fluid particles by swimming bodies, which viscous effects can lengthen, is more relevant to stirring than the scale of turbulence they produce. This is the viewpoint adopted in this Letter.

Huntley and Zhou [7] considered the energy produced by 11 representative species of schooling animals, from krill to whales, and found that regardless of size the energy input to the ocean per unit mass from the swimming of these animals was roughly a constant of order 10^{-5} W/kg. If the average the biomass of the oceans has a volume fraction c over a volume V in cubic meters, we can thus (assuming biological materials have the density of water) arrive at a total energy input of $10^{-2}cV$ W. The area of the oceans is about 3.6×10^{14} m^2, and if we assume the biomass is evenly distributed to a depth D meters, we get an input of $3.6Dc \times 10^{12}$ W. This suggests that for a typical depth of one kilometer the volume density of biomass should be of order 10^{-3}–10^{-4}, and thus that the organisms form a dilute suspension, even if their distribution is patchy and organized into schools.

The object of the present Letter is to determine the effective diffusivity and the statistics of the concentration field of a passive scalar that can result from the fluid motions caused by such dilute arrangements of swimming animals. The scalar could be for example heat, salt, or nutrients, and is assumed to have negligible feedback on the flow (at least at small scales). The animals considered by Dewar et al. [2] and Huntley and Zhou [7] have large Reynolds number, typically 10^2–10^7. Our focus is therefore distinct from the mixing that can occur from dense, tightly interacting suspensions of Stokesian swimmers, as in [8–13], though it shares many common features such as linearity in the density of swimmers. Real swimmers present a wide variety of motions and wakes, but these have generic forms in the far field [14]. For example, the far potential field of a neutrally buoyant fish in steady unaccelerated swimming decays at least like a quadrapole. Following [6], we will model the swimmers by identical cylinders or spheres moving in potential flow, but these are merely stand-in examples. We emphasize that though the motivating application comes from oceanography, the simple model we introduce can be applied to a range of systems, such as the mixing caused by vortices or suspensions of solid particles.

Dilute suspensions of swimmers. As an extremely simple model of stirring by swimmers, we consider a fluid particle, called the target particle, which is influenced by the occasional passing of swimming bodies. We assume that every swimmer moves at a fixed speed U, over distances $\mathrm{O}(L)$ large compared to the "range of in-

* Corresponding author at: Department of Mathematics, University of Wisconsin – Madison, 480 Lincoln Dr., Madison, WI 53706, USA.
E-mail address: jeanluc@math.wisc.edu (J.-L. Thiffeault).

0375-9601/$ – see front matter
doi:10.1016/j.physleta.2010.06.043

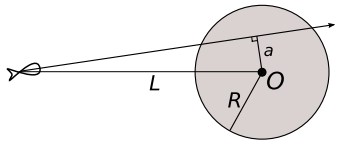

Fig. 1. A swimmer coming a distance a from a particle at O.

fluence". This range will typically be a few body lengths normal to the swimming path, and represents the distance from a target particle where interaction with the swimmer becomes significant. We assume that encounters of our target particle with swimmers are occasional, in that at each encounter the particle moves by a distance $\Delta(a)$, where the impact parameter a is the perpendicular distance of the initially unperturbed particle from the extended line of motion of the approaching swimmer. Since we are assuming that L is large compared to the distance of significant interaction, we may assume that by an "encounter" we mean that the $\Delta(a)$ may be computed from motion of the swimmer along a doubly-infinite line. Each encounter, the kth say, moves the particle a distance $\Delta(a_k)$, in the direction of the unit vector $\hat{\boldsymbol{r}}_k$. Thus after M encounters the position of a target particle initially at $\boldsymbol{x}_0$ is $\boldsymbol{x}_M$ given by

$$\boldsymbol{x}_M = \boldsymbol{x}_0 + \sum_{k=1}^{M} \Delta(a_k)\hat{\boldsymbol{r}}_k. \tag{1}$$

Assuming infrequent encounters, we regard the $a_k, \hat{\boldsymbol{r}}_k$ as independent and identically distributed random variables. We then follow Einstein's derivation [15] for computing the displacement,

$$\langle |\boldsymbol{x}|^2 \rangle = M\langle \Delta^2(a) \rangle + \left\langle \sum_{j\neq k} \Delta(a_j)\Delta(a_k)\hat{\boldsymbol{r}}_j \cdot \hat{\boldsymbol{r}}_k \right\rangle, \tag{2}$$

where we assume spatial homogeneity to set $\boldsymbol{x}_0 = 0$, and the angle brackets denote ensemble averaging. The $\hat{\boldsymbol{r}}_k$ are isotropically distributed, so the second term above vanishes.

To evaluate $M\langle\Delta^2(a)\rangle$, consider a swimmer at a large distance L from the target particle at the origin O (see Fig. 1). Imagine a "target disk" (or sphere in 3D) of radius R, with $\ell \ll R \ll L$, where ℓ is a typical length scale for the swimmer. The fraction of swimmers that will hit the target disk (sphere) is $2R/2\pi L$ ($\pi R^2/4\pi L^2$ in 3D). We can use the number density and the volume of the 'shell' at a distance L to find that the number of swimmers hitting the target from a distance L is $2Rn\,dL$ ($\pi R^2 n\,dL$ in 3D), where n is the number density of swimmers. We now integrate from 0 to Ut, since swimmers further than Ut cannot hit the target, to find the number of swimmers M that will hit the interaction disk (sphere) in time t: we find $M = 2RUnt$ ($M = \pi R^2 Unt$ in 3D). The expression for the squared displacement (2) is now

$$\langle |\boldsymbol{x}|^2 \rangle = M \int_0^R \rho(a)\Delta^2(a)\,da$$

since the largest value of the impact parameter is R. Here $\rho(a)$ is the probability distribution of impact parameters; since the swimmers are assumed to arrive from far away, this is $\rho(a) = 1/R$ ($\rho(a) = 2\pi a/\pi R^2$ in 3D). Combining these results and taking $R \to \infty$, we find

$$\langle |\boldsymbol{x}|^2 \rangle = \begin{cases} 2Unt \int_0^\infty \Delta^2(a)\,da & \text{(2D)}; \\ 2\pi Unt \int_0^\infty a\Delta^2(a)\,da & \text{(3D)}, \end{cases} \tag{3}$$

assuming that the integrals converge. Since the effective diffusivity κ is defined by $\langle |\boldsymbol{x}|^2 \rangle = 2d\kappa t$, with d the spatial dimension, Eq. (3) can be used to determine κ.

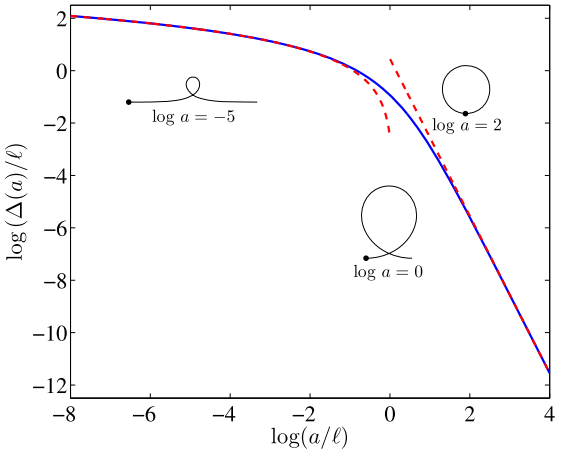

Fig. 2. Displacement $\Delta(a)$ due to a cylinder, as a function of the impact parameter a. The dashed lines are the asymptotic forms for small and large a of Eq. (5). A few typical trajectories are overlaid: for large a the trajectory is almost circular, but is still ribbon-shaped.

Displacement due to a moving body. To find the displacement $\Delta(a)$ of a target particle due to a swimming body coming from infinitely far away and swimming in the z direction, we need to integrate the equations for the position of a target particle at $\boldsymbol{x}(t)$,

$$\dot{\boldsymbol{x}} = \boldsymbol{u}(\boldsymbol{x}, t), \qquad \boldsymbol{x}(-\infty) = (a, 0, -\infty) \tag{4}$$

for t ranging from $-\infty$ to ∞. The impact parameter, a, appears as the initial horizontal position of the target particle. This classical 'drift' problem has been treated in great detail by many authors; see for example [16–19].

As a working example of the displacement due to a moving body, we shall first treat the circular cylinder. We consider the displacement in two-dimensional flow due to the passage of a cylinder of radius ℓ moving at speed U in potential flow. Eq. (4) can be integrated numerically for a given a to obtain $\Delta(a)$, plotted in Fig. 2. The characteristic 'ribbon' shape is evident. Also shown are the asymptotic forms [17]

$$\Delta(a)/\ell \sim \begin{cases} \log(\ell/a) + .0794, & a \ll \ell; \\ \pi(\ell/a)^3/2, & a \gg \ell. \end{cases} \tag{5}$$

There is an integrable logarithmic singularity for small a. For large a, the trajectories are almost circles. By combining these asymptotic limits with numerical integration, we find the integral from Eq. (3) is $\int_0^\infty \Delta^2(a)\,da \simeq 2.37\ell^3$. But note that $\int_0^\ell \Delta^2(a)\,da \simeq 2.31\ell^3$: the integral is completely dominated by "head-on" collisions (97% of the integral).

For a sphere in three-dimensional potential flow, the displacement $\Delta(a)$ appears superficially much as for the cylinder in Fig. 2, but drops off more rapidly for large a:

$$\Delta(a)/\ell \sim \begin{cases} \frac{4}{3}\log(\ell/a) - .582, & a \ll \ell; \\ 9\pi(\ell/a)^5/64, & a \gg \ell. \end{cases} \tag{6}$$

As for the cylinder, there is an integrable logarithmic singularity for small a, and the integral in Eq. (3) is $\int_0^\infty a\Delta^2(a)\,da \simeq .254\ell^4$. The small a logarithmic singularity is mollified by the extra factor of a in the integral, but still $\int_0^\ell a\Delta^2(a)\,da \simeq .250\ell^4$: as it was for the cylinder, the integral is completely dominated by "head-on" collisions (98% of the integral), due to the rapid decay of the displacement with impact parameter. For both the cylinders and spheres, the logarithmic singularity is the dominant contribution to the integral. The coefficient of the logarithm in Eqs. (5) and (6) is given by the linearized flow near the stagnation points at the front and rear of the cylinder or sphere, suggesting that the integral is

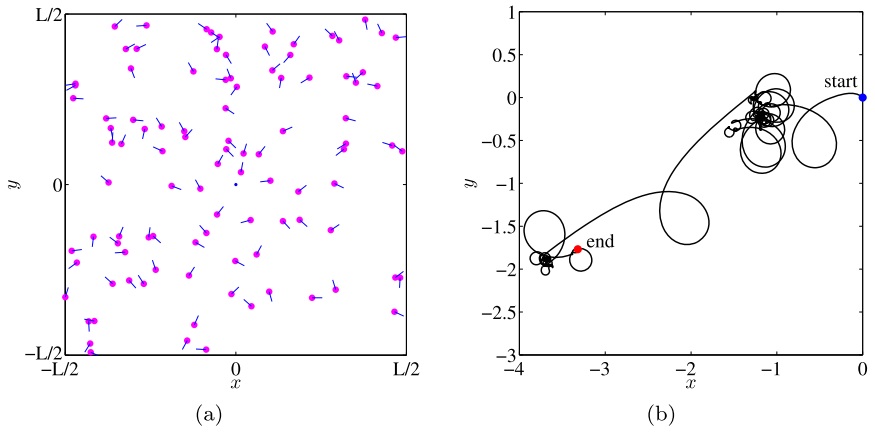

Fig. 3. (a) Initial configuration of $N = 100$ cylinders moving at constant speed $U = 1$ in random directions. Each cylinder has radius $\ell = 1$ and the periodic box size used in the simulation is $L = 1000$ (cylinders not to scale). (b) Trajectory of target particle, initially at the origin, integrated for 10^5 time units.

easy to approximate for more complicated swimmers. Putting all the numerical factors together, we find the effective diffusivity

$$\kappa = \begin{cases} 1.19Un\ell^3 & \text{(cylinders)}; \\ .266Un\ell^4 & \text{(spheres)}. \end{cases} \tag{7}$$

We can justify these formulas dimensionally by observing that the frequency of collisions is linear in both U and n, and since we are assuming the path length is infinite the only other length scale is the swimmer size ℓ.

Direct simulation of dilute suspensions. To validate our theoretical predictions, we consider 2D swimmers moving in straight lines within the square $\mathcal{S}$: $-\frac{1}{2}L \leqslant x, y \leqslant \frac{1}{2}L$. We assume each swimmer is a cylinder of radius $\ell = 1$, with $L \gg \ell$. We initially place N swimmers at random positions within $\mathcal{S}$, which subsequently move with unit speed in a random direction. (Fig. 3(a) shows a typical initial configuration.) Positions are subsequently computed mod L in both directions, maintaining the number density n in $\mathcal{S}$. Diluteness requires that $n\ell^2 \ll 1$. A target particle initially at the origin moves under the potential flow created by all of the cylinders. Since the cylinders are typically well-separated, we compute their net velocity field by linear superposition. We show an example of this computation in Fig. 3(b), for the values $L = 1000$, $n = 10^{-4}$. The larger "ribbons" caused by drift are easily identified, suggesting that in this dilute limit the approximation of encounters as being independent will hold.

Fig. 4 shows the mean-squared displacement $\langle|\boldsymbol{x}|^2\rangle$ of a target particle over 2×10^6 trials (realizations) for $N = 10$ cylinders, again with unit radius and speed. The solid line confirms that $\langle|\boldsymbol{x}|^2\rangle$ grows linearly with time, and the dashed line shows the 2D theoretical prediction (7) for cylinders. The discrepancy is due to Eq. (7) only being valid in the limit of infinite dilution, i.e., as $n\ell^2 \to 0$. We have verified that as the dilution is increased the slope approaches the theoretical prediction. The mean is dominated by a few trajectories with large displacements, corresponding to small impact parameter a. Analogous remarks apply to a suspension of spheres in three dimensions: the theoretical predictions are verified there as well.

Typical physical values. We will use values for typical krill as in [4]. We consider spheres of radius $\ell = 1$ cm, swimming speed $U = 5$ cm/sec, and number density $n = 5\times10^{-3}$ cm^{-3}. Eq. (7) then gives an effective diffusivity of 7×10^{-3} cm^2/sec, about five times the thermal molecular value 1.5×10^{-3} cm^2/sec, and five hundred times the molecular value 1.6×10^{-5} cm^2/sec for salt. This implies a considerable enhancement to the molecular diffusion, but we emphasize that these values apply within a school of krill: the distribution and size of the schools themselves is a more complicated matter [7]. Note also that a small change in the

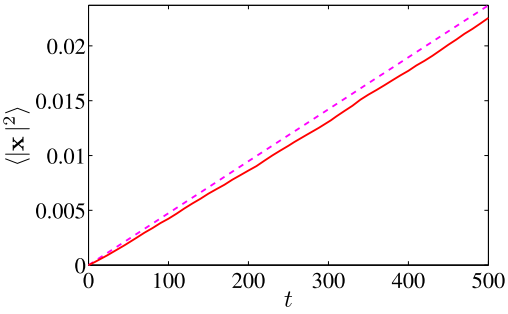

Fig. 4. The mean-squared displacement (solid line) of a target particle for 2×10^6 realizations of $N = 10$ cylinders, with otherwise the same parameters as in the caption to Fig. 3(a). The dashed line shows the squared displacement predicted by Eqs. (3) and (7), using a number density $n = 10^{-5}$. The discrepancy between the two lines is due to (7) being valid in the limit of infinite dilution.

swimmer size has a huge impact: for a radius of .5 cm, the effective diffusivity is 4×10^{-4} cm^2/sec, an order of magnitude smaller than for 1 cm. If we use mean densities as discussed in the introduction, the effective diffusivity decreases by a factor of 10 to 100.

Effect of viscosity. We expect viscosity to greatly enhance κ. This will be the focus of future investigation, but for now we present a rough estimate of the impact of viscous no-slip boundary conditions at the surface of the swimmer. For inviscid flow, the displacement function $\Delta(a)$ has a logarithmic singularity near the axis of swimming; for viscous flow near a no-slip boundary, the displacement function has the stronger singularity

$$\Delta(a) \sim C\ell^2/a, \quad a \ll \ell, \tag{8}$$

where $C = \sqrt{2/3}\pi$ for a sphere of radius ℓ [20,21]. This implies that the 3D squared-displacement integral in (3) diverges as $a \to 0$. The divergence of the second moment $\langle|\boldsymbol{x}|^2\rangle$ is often associated with Levy flights, but here we are interested in scales that are much larger than the typical correlation length of swimming, i.e., the typical length λ for which a swimmer travels roughly in a straight line before changing direction. We thus expect the overall long-time transport to remain diffusive, and we can cap-off the displacement function at a maximum value λ. In other words, a particle which is directly in the path of a swimmer cannot travel further than the swimmer itself: this regularizes the integral (3) to give

$$\langle|\boldsymbol{x}|^2\rangle \simeq 2\pi Unt \int_{C\ell^2/\lambda}^{\infty} a\Delta^2(a)\,da \tag{9}$$

where the lower bound of the integral is the value at which the displacement (8) achieves its maximum allowable value, λ. We introduce a transition length scale where we switch from the boundary-layer form $\Delta \sim a^{-1}$ to the inviscid form derived earlier, and find again that the dominant contribution to the integral arises from small a, as was the case for potential flow, yielding

$$\kappa \simeq \tfrac{\pi}{3} U n \ell^4 C^2 \log(\lambda/\ell). \tag{10}$$

For spheres, this is $\kappa \simeq (2\pi^3/9) U n \ell^4 \log(\lambda/\ell) = 6.89 U n \ell^4 \log(\lambda/\ell)$. Inserting the same numerical values for krill as before, with a path length $\lambda = 100$ cm, we find $\kappa \simeq .8$ cm^2/sec, about 500 times the molecular value. Thus, including the effect of viscosity and finite path length has increased the effective diffusivity by a factor of 100 over the inviscid flow case. We emphasize that this is a rough estimate. The path length (or swimming correlation length) is a measure of how much a swimmer tends to move in one direction before turning. Our chosen value of 1 m is not based on any evidence, but κ has only a weak logarithmic dependence on λ. Assuming a value $\lambda = 10$ m only raises κ from .8 to 1.2 cm^2/sec.

Any conclusion regarding the importance of biomixing in the oceans must be carefully qualified: at the densities inside of schools, the inclusion of viscous effects suggests a rather large enhanced diffusivity, comparable with other processes [1], while outside of schools the effect is much weaker. However, our viscous estimate is rough and more effects will need to be included to form a complete theory: boundary layers, more realistic shape distributions for the swimming bodies, wakes, spatial correlations between the swimmers, patchiness and schooling, finite correlation length of swimming, distribution of velocities, and buoyancy and stratification effects. This last item is probably the most important: stratification can cause fluid parcels to return to their initial height after being displaced if they can't equilibrate their density with their surroundings. A mechanism such as enhanced diffusion due to small-scale turbulence might assist this equilibration.

The simplicity of our model means that prefactors and scalings can be computed accurately. The numerical constants we obtained depend mostly on the flow near the stagnation points around the swimming body. Our simple model can serve as a platform on which to build complexity, or could be applied to other fluid-dynamical systems where a collection of objects causes mixing, such as in sedimentation.

Acknowledgements

The authors are grateful to W. Dewar, R. Ferrari, M. Graham, Z.G. Lin, C. Ortiz–Duenas, Y.-K. Tsang, and W. Young for helpful discussions, as well as to the hospitality of the 2008 Summer Program in Geophysical Fluid Dynamics (supported by NSF and ONR) at WHOI, where this work began, and the Institute for Mathematics and its Applications (supported by NSF). S.C. was supported by NSF under grant DMS-0507615, J.-L.T. under grant DMS-0806821.

References

[1] W.H. Munk, Deep-Sea Res. 13 (1966) 707.
[2] W.K. Dewar, R.J. Bingham, R.L. Iverson, D.P. Nowacek, L.C.St. Laurent, P.H. Wiebe, J. Mar. Res. 64 (2006) 541.
[3] E. Kunze, J.F. Dower, I. Beveridge, R. Dewey, K.P. Bartlett, Science 313 (2006) 1768.
[4] A.W. Visser, Science 316 (5826) (2007) 838.
[5] M.C. Gregg, J.K. Horne, J. Phys. Oceanogr. 39 (2009) 1097.
[6] K. Katija, J.O. Dabiri, Nature 460 (2009) 624.
[7] M.E. Huntley, M. Zhou, Mar. Ecol. Prog. Ser. 273 (2004) 65.
[8] T.J. Pedley, J.O. Kessler, Annu. Rev. Fluid Mech. 24 (1992) 313.
[9] X.-L. Wu, A. Libchaber, Phys. Rev. Lett. 84 (2000) 3017.
[10] J.P. Hernandez-Ortiz, C.G. Dtolz, M.D. Graham, Phys. Rev. Lett. 95 (2006) 204501.
[11] D. Saintillian, M.J. Shelley, Phys. Rev. Lett. 99 (2007) 058102.
[12] P.T. Underhill, J.P. Hernandez-Ortiz, M.D. Graham, Phys. Rev. Lett. 100 (2008) 248101.
[13] K.C. Leptos, J.S. Guasto, J.P. Gollub, A.I. Pesci, R.E. Goldstein, Phys. Rev. Lett. 103 (2009) 198103.
[14] M.J. Lighthill, Hydrodynamic far fields, in: T. Miloh (Ed.), Mathematical Approaches in Hydrodynamics, Society for Industrial and Applied Mathematics, Philadelphia, PA, 1991, pp. 3–20.
[15] A. Einstein, Investigations on the Theory of the Brownian Movement, Dover, New York, 1956.
[16] J.C. Maxwell, Proc. London Math. Soc. 1–3 (1) (1869) 82.
[17] C.G. Darwin, Proc. Cambridge Philos. Soc. 49 (2) (1953) 342.
[18] I. Eames, S.E. Belcher, J.C.R. Hunt, J. Fluid Mech. 275 (1994) 201.
[19] I. Eames, J.W.M. Bush, Proc. R. Soc. London Ser. A 455 (1999) 3665.
[20] W.R. Young, S.W. Jones, Phys. Fluids A 3 (10) (1991) 2468.
[21] I. Eames, D. Gobby, S.B. Dalziel, J. Fluid Mech. 485 (2003) 67.